World Academics Journal of Engineering Sciences
Vol.7, Issue.1, pp.66-72, March (2020)

Research Paper

E-ISSN: 2348-635X

Ecological Evaluation of Urban Heat Island Impacts in Abuja Municipal Area of FCT Abuja, Nigeria

Thomas .U. Omali

National Biotechnology Development Agency (NABDA), Fed. Min. of Sci. & Tech., Abuja, Nigeria

Available online at: www.isroset.org

Received: 02/Mar/2020, Accepted: 31/Mar/2020, Online: 10/Apr/2020

***Abstract*—**The rate of urbanization in recent time has increased due to ever-increasing population density, which usually culminates in the modification of land use/cover (LULC) structure. This change in LULC give rise to the increase in impervious surface cover, which causes Urban Heat Island (UHI) due to alteration in the thermal characteristics of the urbanized area. The purpose of this study is to conduct a spatiotemporal estimation of Urban Heat Island (UHI) effects in Abuja Municipal Area Council (AMAC) of FCT Abuja, Nigeria for 1987, 2001, and 2016. This was achieved by the computation of Normalized Difference Vegetation Index (NDVI), Land Surface Temperature (LST), and Urban Thermal Field Variance Index (UTFVI). The UTFVI was eventually used to express the UHI impacts in the study area based on ecological evaluation index classes (1-6). Finally, the results from the study reveal that there is no UHI effect in classes 4-6 throughout the study epoch while class 3 of 2016 indicates strong UHI, and classes 1 to 3 of 1987 and 2001, as well as classes 1 and 2 of 2016 exhibit the strongest UHI.

Keywords*—*Index, landsat, LST, microclimate, remote sensing, UTFVI

I. INTRODUCTION

Metropolitan settlements are the most significant human settings that can be linked to the processes of urbanization. The global human population in urban centres have been increasing at various percentage of the entire global population. For example, it was 13 percent in 1900, 29 percent in 1950, 49 percent in 2005, and it is estimated to be 60 percent in 2030 [1]. Consequently, there is a concerted utilization of the cities, and incessant effects on the inhabited environment. Moreover, the contemporary escalating rate of urbanization usually culminates in alterations of land use and land cover most especially in the developing nations. Natural vegetation and soil are now giving way for other land use and land cover, which portray urban structures. This is usually accompanied with associated impact, most particularly with regards to the modifications in the factors that are responsible for land surface energy exchange including albedo, emissivity, and heat capacity.

The high temperature usually experienced in cities is the consequence of physical aspects of urban landscape, anthropogenic heat contribution, and meteorological conditions [2-3]. The physical presence of cities modifies the radiative, aerodynamic, thermal, as well as the moisture properties of the atmosphere within and around urban centres, and the most evident consequence is that of positive thermal anomalies connected with nocturnal urban air temperature. The high rate at which energy is being used is contributing significantly to the release of gases into the atmosphere, which alters the near-surface thermal ray flux and the microclimate of urban areas. This modification demonstrates the climatic disparity between urban settlements and their neighbouring rural areas, which is generally referred to as the Urban Heat Island (UHI) impact.

UHI is the usual warming of the cities as compared to their neighbouring area [4]. It is a unique occurrence of urban ecological unit which describe a familiar feature of human-induced impacts on air temperature, and also exert significant effect on global climate warming [5]. Simply, this phenomenon is a reflection of the entirety of microclimatic alterations resulting from urbanization [6]. Of course, the warming of air temperature is likely to exert some adverse impacts on the environment, as well as the socioeconomic activities [7].

UHI and their behaviour can be evaluated by using either the air or surface temperature measurements. Nowadays, thermal infrared wave bands have become an essential means to study the UHI [8] as they are used to retrieve Land Surface Temperature (LST) [9]. Various researchers have acknowledged the use of remote sensing data in retrieving LST and UHI including [10-20]. The current study is a similar effort through which the UHI effect is analyzed from 1987 to 2016 for Abuja Municipal Area Council, Federal Capital Territory Abuja, Nigeria. It was achieved by using the thermal bands of Landsat datasets to derive the LST of the study area over the study period. Finally, the Urban Thermal Field Variance Index (UTFVI) was computed from the LST and was used to determine the rate of UHI effect with regards to ecological evaluation index.

II. STUDY AREA

Abuja Municipal Area Council is located in the east of Federal Capital Territory, Abuja. It lies between latitudes

8˚37'41" and 9˚9'15" north of the equator, and longitudes 7˚03'55" and 7˚34' 00" east of the Greenwich Meridian (figure 1). Also, AMAC is the largest and most developed of the six area councils in the FCT as evidenced by its landmass of approximately 1608.487 km^2.

The study area is topographically characterized by a blend of hilly and leveled land surface. This is demonstrated by numerous hills and rocks especially in Jahi, Maitama, Asokoro, Wuye and Apo, while other areas are characterized by slopes such as Gwarinpa, Mpape and others. Like every other location in Abuja, the study area is composed of hot, humid, and tropical climatic condition and it falls within the guinea savanna ecological zone with its main vegetation being categorized into grass, woodland, and shrub.

The general increasing human population and urban sprawl in the FCT Abuja results in the emergence of satellite towns and smaller settlements. Consequently, there has being a corresponding loss of vegetation which exerts a substantial influence on the micro-climate of the area.

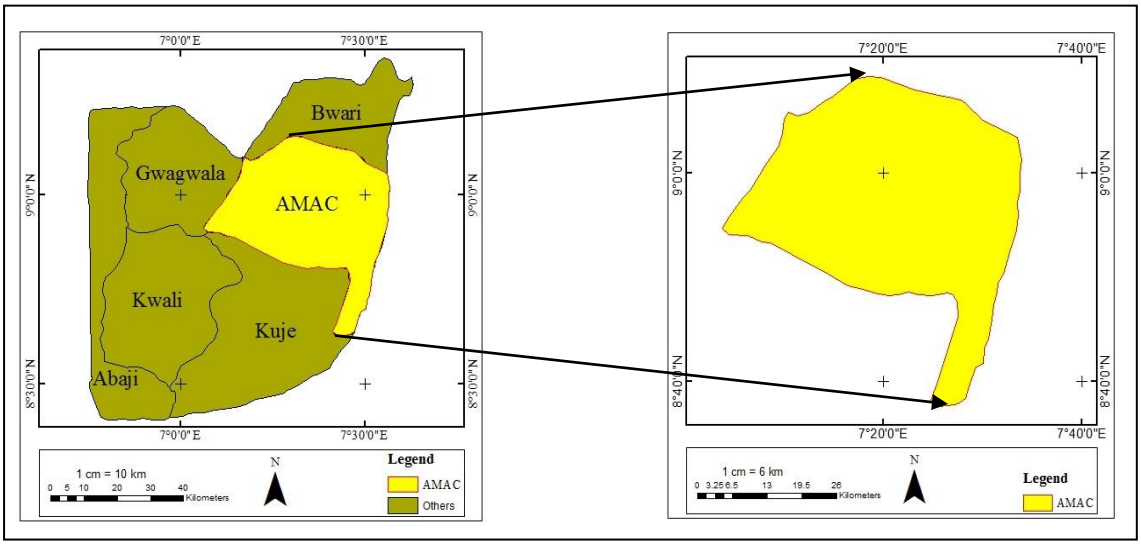

Fig. 1: Location map of the study area.

III. METHODOLOGY

3.1. Data Acquisition

This study utilized Landsat imageries (table 1) covering the study area (path 189, row 054). They were acquired for the period of the study from the USGS through the Earth explorer (www.earthexplorer.com). However, only the thermal bands of the satellite data were utilized for the study. The landsat thermal bands include band 6 for TM and ETM+, and band 10 and 11 for OLI/TIR.

3.2. Image Preprocessing

The purpose of image pre-processing is to produce enhanced satellite images before its final processing and analysis. Image pre-processing performed in the current study includes image enhancement, geometric rectification, topographic correction as well as radiometric and atmospheric calibrations [21].

Radiometric calibration was performed to correct the sensitivity of the remote sensor, topography, sun angle. Also, geometric correction was carried out so as to precisely fix the images to a particular coordinate system, that is, WGS 1984.

Atmospheric correction was also performed to eliminate the error caused by atmospheric scattering, absorption and reflection. Finally, the images were resampled because the resolution of the thermal band is different to other bands. For landsat TM and ETM+, the resolution of thermal band (band 6) are 120 m, 60 m respectively, and that of OLI/TIR (bands 10 and 11) is 100 m, while the resolution of the rest other bands is 30 m.

Table 1: Satellite data used for the current study

Data Type	Path/Row	Data Sources	Date Acquired	Resolution
Landsat TM	189/054	USGS	1987-12-21	30m
Landsat ETM+	189/054	USGS	2001-12-27	30m
Landsat OLI/TIR	189/054	USGS	2016-12-28	30m

3.3. Normalized Difference Vegetation Index

NDV has advantages, such as lower influence of atmospheric variations, greater sensitivity to chlorophyll, and reduction of noise by normalization. For this reason, it is commonly used to determine the spatial extent and healthiness of vegetation cover. In the current study, it was

determined through a sequence of computation by using the visible red and near infrared (NIR) channels of the satellite imageries [22] through equation (1). For NDVI, the reflectance of healthy vegetation is high and low in the near infrared and the red bands respectively, thus enhancing the analysis of vegetation while subduing subtle noise from other land cover types.

NDVI= (NIR-RED)/ (NIR-RED) ……..…… (1)

Where NIR and RED are reflectance corresponding to bands 4 and 3 respectively for Landsat 7, and other Landsat prior to 7. For landsat 8 however, the NIR and RED radiation match with channels 5 and 4 respectively.

The computation of NDVI serves two main purposes in this study. Its values reveal whether the land cover is vegetation, which has a cooling influence on land surface temperature; hence it is adopted for the UHI effect mitigation. Moreover, emissivity values were derived from satellite-based NDVI.

3.4. Land Surface Temperature

Land surface temperature (LST) is a very important factor in various areas of research such as global climate change, urban land use/land cover, and geophysical as well as biophysical studies. Estimating LST from landsat 5 and 7 images is straight forward. On the other hand, there are three main ways to estimate LST from Landsat 8 data: the radiative-transfer equation, the split-window (SW) algorithm, and the single-channel (SC) technique. The USGS suggested the use of TIRS Band 10 only, which has fewer expected errors caused by stray light anomalies compared to Band 11 (before 24 April 2017). For the current study, LST was retrieved from geometrically corrected thermal bands of the satellite imageries using the following sequence:

First, spectral radiance was calculated (for Landsat 5) using the following equation:

L=Lmin + (Lmax-Lmin) *DN/255..…… (2)

Where L is Spectral Radiance, DN is Digital Number, and the values of Lmin and Lmax are documented in the metadata.

Second, radiation luminance was converted to at-satellite brightness temperature in Kelvin T (K), by using the following equation [23]:

BT=K2/ (lnK1/L+1)…...…….. (3)

Where, K1 and K2 are calibration constants documented in the metadata, BT = Brightness Temperature.

Third, the Kelvin-Celsius conversion was done as follows:

T (ºC) = TB - 273.15..…….…….…… (4)

Fourth, the NDVI was used to calculate the proportion of vegetation (Pv) using equation (5) [24].

$$Pv = (NDVI - NDVI_{MIN}) / (NDVI_{MAX} - NDVI_{MIN}) \ldots. (5)$$

Where Pv is portion of vegetation, NDVI is Normalized Difference Vegetation Index, $NDVI_{MIN}$ is minimum NDVI, and $NDVI_{MAX}$ is maximum NDVI.

Fifth, the emissivity values are critical parameters for modeling LST from satellite image. Emissivity (ε) is a proportionality factor, which is used to scale blackbody radiance to predict emitted radiance (Planck's law). It is the efficiency of transmitting thermal energy across the surface into the atmosphere. The land surface emissivity is calculated by using the following equation [25].

ε = 0.004*Pv*0.986.……..…..…… (6)

Where ε is emissivity and Pv is represent the proportion of vegetation.

Sixth, at this stage, equation 7 was used for LST estimation and derivation of temperature map.

LST= (BT/ (1+0.00115 * BT /1.4388) * Ln(ε)...(7)

Where LST is Land Surface Temperature, BT is the Brightness Temperature, and ε is emissivity.

3.5. Urban Thermal Field Variance Index

Several researchers have used various thermal indices for studying the UHI impacts. These include Temperature Humidity Index (THI) [26], Urban Thermal Field Variance Index (UTFVI) [12] and Wet-bulb Globe temperature (WBGT) [27]. The UTFVI was used in the present study. The UTFVI measures urban ecological quality of life in terms of the degree of thermal comfort in relatively to the existence of the UHI phenomenon. Therefore, it was used to detect varying impacts of the UHI in the study area. In order to illustrate the level UHI impact more clearly, the result of UTFVI were categorized into six classes (Table 2) [28], and each category correspond to a fixed ecological evaluation index (EEI). UTFVI is frequently used to show UHI effect. It was calculate using the following model [29]:

$$UTFVI = (T_s - T_{mean}) / T_s \ldots\ldots (8)$$

Where, T_s is the LST in certain point of the map and T_{mean} is the corresponding mean temperature of the whole area.

Table 2: Threshold of ecological evaluation index

UTFVI	UHI	EEI
< 0	None	Excellent
0.000–0.005	Weak	Good
0.005–0.010	Middle	Normal
0.010–0.015	Strong	Bad
0.015–0.020	Stronger	Worse
> 0.020	Strongest	Worst

VI. RESULTS AND DISCUSSION

The essential parameters used in this study for the assessment of Urban Heat Island effects in the study area are depicted in figures 2-7, and tables 3 and 4. Specifically, figures 2-4 show the LST results, while figures 5-7 show the results of UTFVI. Furthermore, table 3 show the values of LST for the study epoch while table 4 depicts the UTFVI values for the same epoch.

The results of LST reveals that the maximum temperature increased from 40.1ºC to 45.1ºC between 1987 and 2001, and declined to 42.1ºC in 2016, while the minimum temperature declined from 21.7 ºC to 16.7ºC between 1987 and 2001, and increased to 21.2 ºC in 2015 (see table 3). It is obvious that as the maximum temperature increases, the minimum temperature reduces, and the reverse is the case. Also, higher temperature appeared more in the central and northern area for the three epochs. These areas are more of the city centre, and are characterized by urban development. Moreover, the spatial extent of higher LST is larger in 2016 as compared to those of 2001 and 1987.

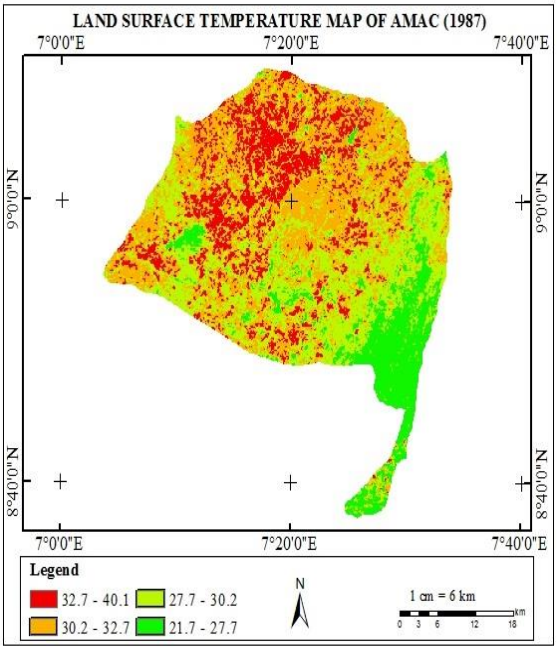

Fig. 2: LST map of AMAC from Landsat of 1987

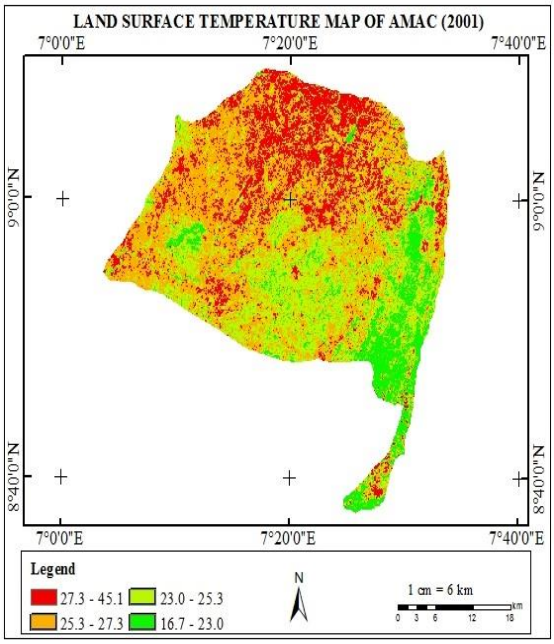

Fig. 3: LST map of AMAC from Landsat of 2001

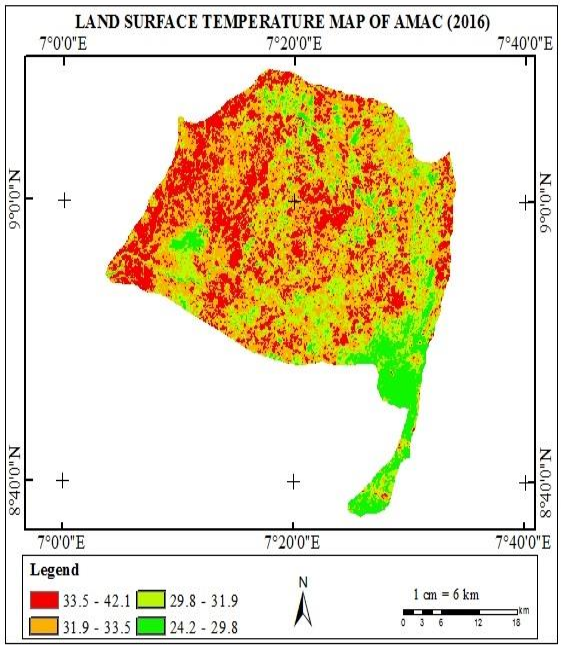

Fig. 4: LST map of AMAC from Landsat of 2016

Table 3: Satellite data used for the current study

LST	1987	2001	2016
Maximum	40.1	45.1	42.1
Minimum	21.7	16.7	24.2

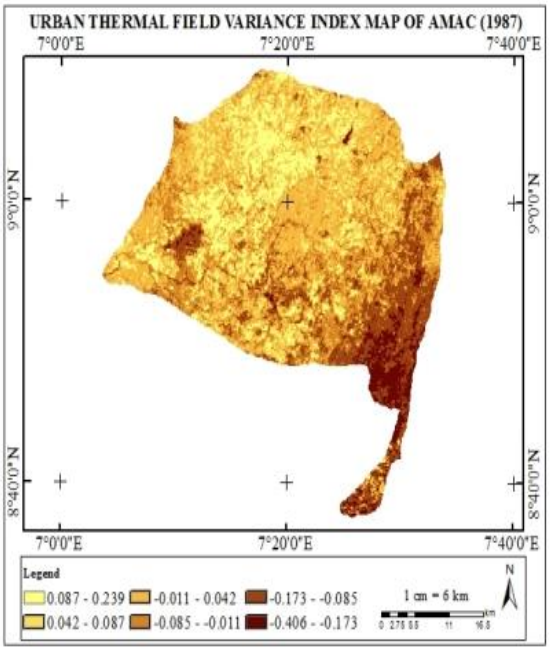

Fig. 5: UTFVI map of AMAC from LST of 1987

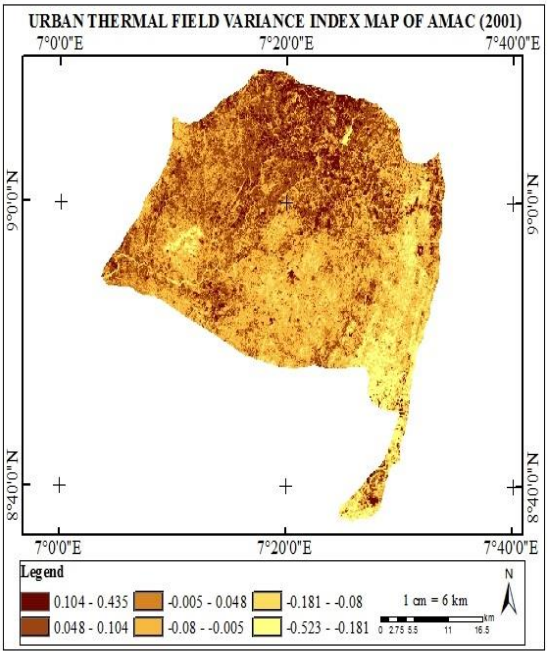

Fig. 6: UTFVI map of AMAC from LST of 2001

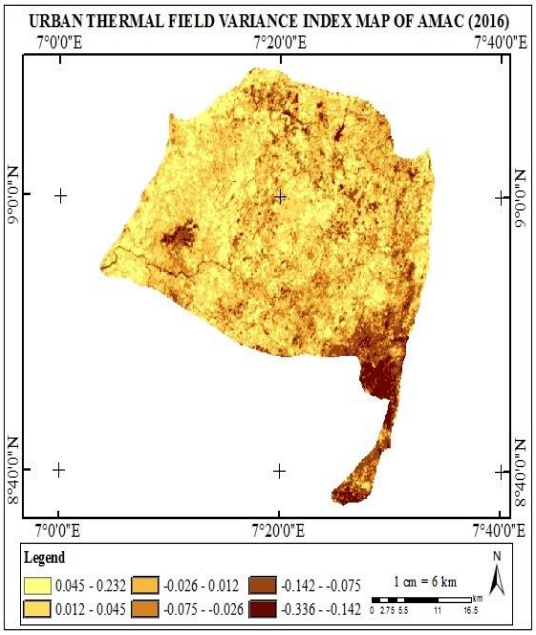

Fig. 7: UTFVI map of AMAC from LST of 2016

The quantitative ecological assessment of UHI impacts in the study area as shown in Figures 5-7 and table 4 depict six classes of UTFVI. When judged with respect to the threshold of ecological evaluation index (table 2), it is apparent that there is no UHI effect in classes 4-6 throughout the study epoch as the highest values of UTFVI for these classes are -0.011, -0.005, and -0.026 for 1987, 2001, and 2016 respectively, that is, they fall below 0 threshold (see table 3). Thus, they can be seen as excellent in terms of ecological evaluation (see table 2). Also, class 3 of 2016 having the maximum UTFVI value of 0.012 indicates strong UHI, which is bad based on ecological evaluation. Furthermore, classes 1 to 3 of 1987 and 2001, as well as classes 1 and 2 of 2016 exhibit the strongest UHI effect judging from their maximum UTFVI values, which are higher than 0.020 thresholds. Therefore, they are ecologically worst.

Similar to the LST, higher UTFVI occurs most in the central and northern area of study for the three epochs. These areas are the most urbanized region of the study area, and thus contain urban structures. Consequently, it causes UHI effects.

Table 4: UTFVI values for AMAC

CLASS	1987		2001		2016	
	$UTFVI_{Min}$	$UTFVI_{Max}$	$UTFVI_{Min}$	$UTFVI_{Max}$	$UTFVI_{Min}$	$UTFVI_{Max}$
1	0.087	0.239	0.104	0.435	0.045	0.232
2	0.042	0.087	0.048	0.104	0.012	0.045
3	-0.011	0.042	-0.005	0.048	-0.026	0.012
4	-0.085	-0.011	-0.080	-0.005	-0.075	-0.026
5	-0.173	-0.085	-0.181	-0.080	-0.142	-0.075
6	-0.406	-0.173	-0.523	-0.181	-0.336	-0.142

V. CONCLUSION

This paper has demonstrated a satellite-based method of monitoring UHI effect. It shows how time series satellite imageries can be used to estimate UHI occurrence as well as the dynamics in UHI impact. The UTFVI which was generated from LST was used to observe the urban ecological quality of life through the connection of thermal comfort and the UHI intensity values.

It is noteworthy that the region in the study area which is impacted by urban heat island effect expanded over the study period, and the highest UHI rising temperature and total amount of UHI rising temperature show a rapid growth in the same period. For this reason, the study area experiences both severe conditions of optimal microclimate for quality urban life and the worst condition of thermal discomfort. Finally, it is evident that satellite remote sensing offers a quicker and efficient technique in the investigation of UHI as compared to the conventional in-situ method.

REFERENCES

[1] Washington DC, New York: Department of Economic and Social Affairs; 2015. United Nations: World Population Prospects: The 2014 Revision United Nations. Available at: www.ncbi.nlm.nih.gov/pmc/articles/PMC5676403

[2] Kleerekoper, L., van Esch, M., Salcedo, T.B., "How to make a city climate-proof, addressing the urban heat island effect,t" *Resour. Conserv. Recycl.*, Vol.**64,** pp.**30–38**, **2012.**

[3] Martin, P., Baudouin, Y., Gachon, P., "An alternative method to characterize the surface urban heat island," *Int. J. Biometeorol.*, Vol.**59,** Issue.**7,** pp.**849–861, 2015.**

[4] Gabriel, K.M., Endlicher, W.R., "Urban and rural mortality rates during heat waves in Berlin and Brandenburg, Germany," *Environ. Pollut.*, Vol.**159,** Issue.**8,** pp.**2044– 2050, 2011.**

[5] Li, X., Mitra, C., Dong, L., Yang, Q., "Understanding land use change impacts on microclimate using Weather Research and Forecasting (WRF) model," *Phys. Chem. Earth*, Vol.**103**, Parts **A/B/C**, pp.**115–126. 2018.**

[6] Alexander, P.J., Mills, G., "Local Climate Classification and Dublin's Urban Heat Island," *Atm.*, Vol.**5,** pp.**755-774, 2014.**

[7] A.I. Hazo, J. Alemak, K. Atiku, A.B. Musa, "Analysis of Trends and Variability in Air Temperature as Evidence of Climate Change in Zaria, Kaduna State, Nigeria," *International Journal of Scientific Research in Multidisciplinary Studies,* Vol.**6**, Issue.**1**, pp.**01-11,2020.**

[8] Keramitsoglou, I., Kiranoudis, C.T., Ceriola, G., Weng, Q., Rajasekar, U., "Identification and analysis of urban surface temperature patterns in Greater Athens, Greece, using MODIS imagery," *Remote Sens. Environ.*, Vol.**115,** Issue.**12,** pp.**3080–3090, 2011.**

[9] Adams, M.P., Smith, P.L., "A systematic approach to model the influence of the type and density of vegetation cover on urban heat using remote sensing," *Landscape and Urban Planning*, pp.**132, 47-54, 2014.**

[10] Giridharan, R., Kolokotroni, M., Urban heat island characteristics in London during winter. *Sol. Energy*, Vol.**83,** pp.**1668–1682, 2009.**

[11] Alexander, B., Wu, J., "Urban heat islands and landscape heterogeneity: linking spatiotemporal variations in surface temperatures to land-cover and socioeconomic patterns," *Landscape Ecol*., Vol.**25,** pp.**17–33, 2010.**

[12] Liu, L., Zhang, Y., "Urban heat island analysis using the Landsat TM data and ASTER data: A case study in Hong Kong," *Remote Sens*., Vol.**3,** pp.**1535–1552, 2011.**

[13] Xiong, Y., Huang, S., Chen, F., Ye, H., Wang, C., Zhu, C., "The impacts of rapid urbanization on the thermal environment: A remote sensing study of Guangzhou, South China," *Remote Sens.*, Vol.**4,** pp.**2033–2056, 2012.**

[14] Clinton, N., Gong, P., "MODIS detected surface urban heat islands and sinks: global locations and controls," *Remote Sens. Environ.*, Vol.**134,** pp.**294–304, 2013.**

[15] Effat, H., Hassan, O., "Change detection of urban heat islands and some related parameters using multi-temporal Landsat images; a case study for Cairo city, Egypt," *Urban Climate*, Vol.**10,** pp.**171–188, 2014.**

[16] Abutaleb, K., Ngie, A., Darwish, A., Ahmed, M., Arafat, S., Ahmed, F., "Assessment of Urban Heat Island using remote sensed imagery over greater Cairo, Egypt," *Adv. Remote Sens.*, Vol.**4,** pp.**35–47, 2015.**

[17] Alfraihat, G., Mulugeta, Gala, T.S., "Ecological evaluation of urban heat island in Chicago city, USA," *Journal of Atmospheric Pollution*, Vol.**4,** Isuue.**1,** pp. **23-29, 2016.**

[18] Bhargava, A., Lakmini, S, Bhargava, S., "Urban Heat Island effect: it's relevance in urban planning," *J Biodivers. Endanger Species*, Vol.**5,** p.**187, 2017.**

[19] Khandelwal, S., Goyal, R., Kaul, N., Mathew, A., "Assessment of land surface temperature variation due to change in elevation of area surrounding Jaipur, India," *Egypt. J. Remote Sensing Space Sci.*, Vol.**21,** Issue,**1,** pp.**87–94, 2018.**

[20] Wang, W., Liu, K., Tang, R., Wang, S., "Remote sensing image-based analysis of the urban heat island effect in Shenzhen, China," *Physics and Chemistry of the Earth*, Vol.**110,** pp.**168–175, 2019.**

[21] Lu, D., Weng, Q., "A survey of image classification methods and techniques for improving classification performance," *Int. J. Remote Sens.*, Vol.**28,** Issue.**5,** pp.**823–870, 2007.**

[22] Okeke, F.I., Omali, T.U., "Spatio–temporal evaluation of forest reserves in the eastern region of Kogi State using geospatial technology," *J. Trop. Environ.,* Vol.**13,** Issue.**1,** pp.**75–88, 2016.**

[23] Van, T.T., Bao, H.D.X., "Study of the impact of urban development on surface temperature using remote sensing in Ho Chi Minh city, north Vietnam," *Geographical Res.* Vol.**48,** Issue.**1,** pp.**86–96, 2010.**

[24] Quintano, C., Fernández-Manso, A., Calvo, L., Marcos, E., Valbuena, L., "Land surface temperature as potential indicator of burn severity in forest Mediterranean ecosystems," *Int. J. Appl. Earth Obs. Geoinf.,* Vol.**36,** pp.**1–12, 2015.**

[25] Sobrino, J.A., Jimenez-Munoz, J.C., Paolini, L., "Land surface temperature retrieval from LANDSAT TM 5," *Remote Sens. Environ.,* Vol.**90,** pp.**434–440, 2004.**

[26] Kakon, A.N., Nobuo, M., Kojima, S., Yoko, T., "Assessment of thermal comfort in respect to building height in a high-density city in the tropics," *Am. J. Eng. Appl. Sci.,* Vol.**3,** Issue.**3,** pp.**545-551, 2010.**

[27] Willett, K.M., Sherwood, S., Exceedance of heat index thresholds for 15 regions under a warming climate using the wet-bulb globe temperature. *Int. J. Climatol.*, 2012, 32(2), 161-177.

[28] Zhang, Y., "Land surface temperature retrieval from CBERS-02 IRMSS thermal infrared data and its applications in quantitative analysis of urban heat island effect," *J. Remote Sens.,* Vol.**10,** pp.**789–797, 2006.**

[29] Liu, L., Zhang, Y., "Urban heat island analysis using the Landsat TM data and ASTER data: A case study in Hong Kong," *Remote Sens.,* Vol.**3,** pp.**1535–1552, 2011.**

